

# Subsurface Mass Rippability Assessment in Basement Environment Using Seismic Refraction Survey

Kouamelan Serge Kouamelan<sup>1\*</sup>, Assi Martial Yapo<sup>1,2</sup>, Koffi Joseph Brou<sup>1</sup>, Eric Thompson Brantson<sup>3</sup>

<sup>1</sup>Laboratoire de Géologie, Ressources Minérales et Energétiques (LGRME), UFR des Sciences de la Terre et des Ressources Minières, Université Felix Houphouët-Boigny, Abidjan, Côte d'Ivoire

<sup>2</sup>Laboratoire du Bâtiment et des Travaux Publics (LBTP), Abidjan, Côte d'Ivoire

<sup>3</sup>Department of Petroleum and Natural Gas Engineering, GNPC School of Petroleum Studies, University of Mines and Technology, Tarkwa, Ghana

Email: \*kouamelan2006@yahoo.fr

**How to cite this paper:** Kouamelan, K.S., Yapo, A.M., Brou, K.J. and Brantson, E.T. (2024) Subsurface Mass Rippability Assessment in Basement Environment Using Seismic Refraction Survey. *International Journal of Geosciences*, 15, 957-966.

<https://doi.org/10.4236/ijg.2024.1512052>

**Received:** October 19, 2024

**Accepted:** December 2, 2024

**Published:** December 5, 2024

Copyright © 2024 by author(s) and Scientific Research Publishing Inc. This work is licensed under the Creative Commons Attribution International License (CC BY 4.0).

<http://creativecommons.org/licenses/by/4.0/>



Open Access

## Abstract

A geophysical investigation was carried out in Kong, northern Côte d'Ivoire, to characterize the subsurface formations as part of a drinking water supply project. The study aimed to determine the seismic signatures of the non-rippable layers and their depths to guarantee the stability of the Kong water reservoir. Based on the analysis of  $V_p$  velocity distribution, the subsoil in the study area is structured into rippable (300 - 1500 m/s), marginal (1500 - 2000 m/s) and non-rippable (>2000 m/s) zones with varying thicknesses. Correlation with core drilling results reveals that the rippable zones, located between 5 and 9 m depth, are associated with the superficial overburden and weathering products (clays and clayey sands), while the non-rippable zones correspond to the very dense granitic basement, located between 5 and 11 m depth according to 2D geoseismic sections.

## Keywords

Seismic Velocity, Level of Rippability, 2D Geoseismic Sections, Water Reservoir, Côte d'Ivoire

## 1. Introduction

The construction of major hydroelectric facilities in a locality is an asset insofar as it contributes to development in general and human advancement in particular

[1]-[5]. They are an essential renewable energy solution for meeting the challenge of electrifying remote rural areas [6].

In drinking and raw water supply projects, the construction of hydroelectric dams, pumping stations and treatment plants requires knowledge of the physical properties of the soil and subsoil. This information on the geological nature and extent of underground structures enables assessing geological and seismic risks, so that preliminary solutions can be envisaged for the foundations and structures required for the projects [7] [8].

Several disasters linked to geology or natural phenomena, such as earthquakes, have affected dams and reservoirs around the world. Disasters due to dam failure are numerous throughout the world [9]-[14]. Structural geology is of prime importance since it helps to obtain as reliable a description as possible of the fault network affecting the siting area, as well as the geodynamic context. The presence of a potentially active fault at a dam or reservoir site should lead to the site being abandoned.

In Côte d'Ivoire, seven dams were built between 1964 and 2017, including the Soubré hydroelectric dam [15]. However, the geological and seismic context of these various dams is little studied and therefore very rare in the literature, sometimes due to the high cost of core drilling. However, knowledge of these parameters can help in understanding the geological framework of other projects located in similar environments.

Indeed, the correlation between seismic tomography and geotechnical studies could be useful for better characterizing the subsoil. This is the vision behind the studies of the site for the construction of a water supply system for the city of Kong and the surrounding area, based on a water reservoir. This study aims to highlight the geological nature of the formations making up the project site, based on a study of the physical properties of the subsoil. It involves determining the seismic characteristics of the granitoids and their alteration profiles on site. This work, based mainly on seismic refraction, will specify the roof of the sound substratum and the ripplable layers of the various horizons.

## 2. Geological Context

Located in the Tchologo region (**Figure 1(a)**), the study area is situated around 8 km from Kong on the Tafiré road and on a tributary of the Kolonkoko River. It belongs to the Eburnian basement and lies on a granitic peneplain that extends south of the Banfora cliff [16]. The area lies to the east of the Sassandra fault and consists mainly of crystalline and metamorphic formations. Lithologically, the region is characterized by Birrimian and granitoid formations, two major groups whose most widespread rocks are essentially granites (**Figure 1(b)**). Granites and migmatites are highly varied and often heterogeneous. They include calc-alkaline granites of various types (muscovite granites, two-mica granites, amphibolite and BioLite granites, granodiorites) and migmatites, which are virtually indistinguishable from Eburnian granites as a source rock.

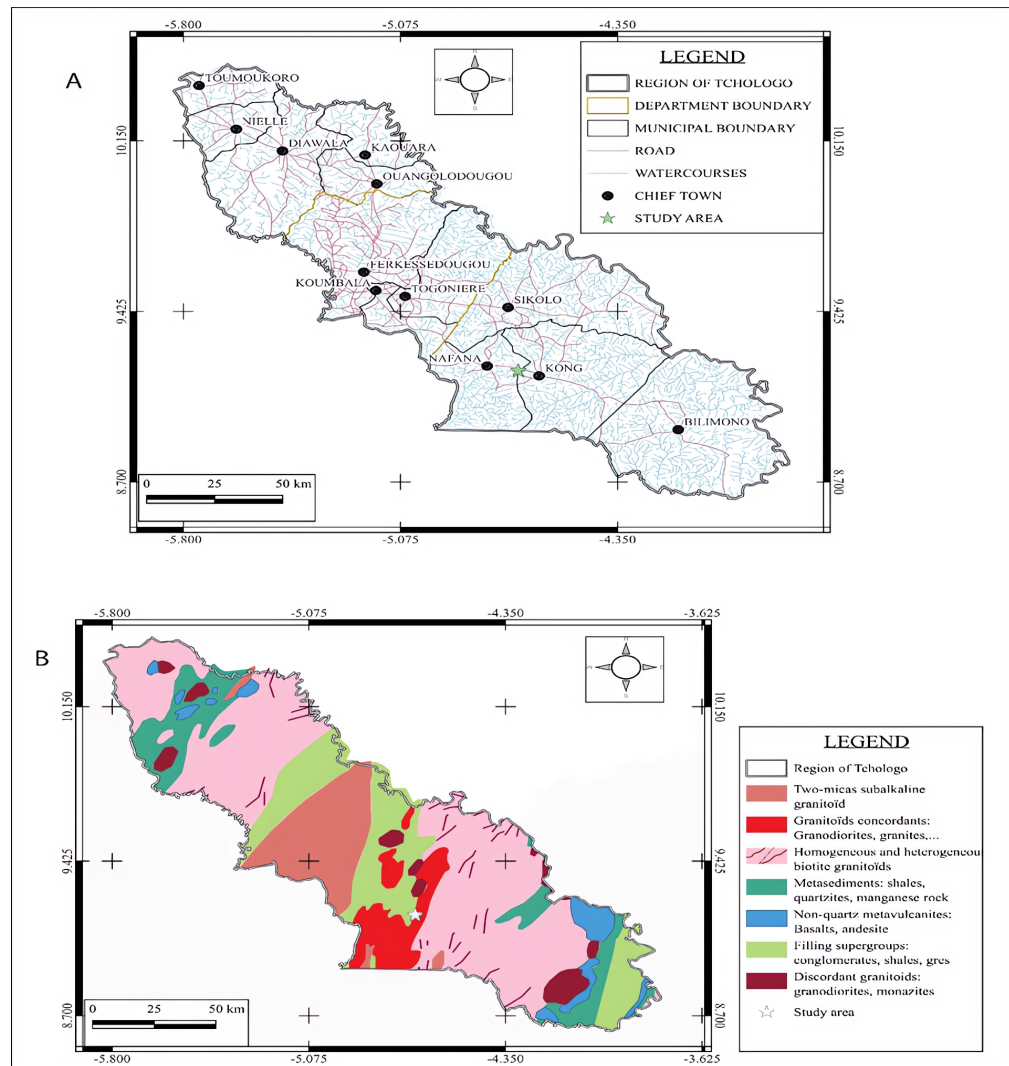


**Figure 1.** Geological map of the Tchologo region showing the geology of Kong.

### 3. Methodology

Four seismic profiles named P0, P1, P2 and P3 were carried out as part of this study (Figure 2). The geometric characteristics of the surveys are shown in Table 1. The technique used is based on measuring the travel time of seismic waves, refracted at the interfaces between underground layers of different velocities (Figure 3). Using a hammer and striking plate, a seismic wave is introduced into the subsoil at the point of impact (S). The energy thus generated propagates underground, either directly through the upper layer (direct arrivals), or laterally down the layers at higher speed (refracted arrivals), before returning to the surface. This energy is detected at the surface by a series of 24 vertical 10 Hz geophones (R). Only the first P-wave arrivals were recorded ( $V_p$ ), providing information on the elastic properties and interface depths of the various geological structures. The acquired data were processed using Rayfract software to resolve lateral changes in depth to the top of a layer and seismic velocities within it.



**Figure 2.** Location of the 4 seismic refraction profiles in the project area. P0 is the baseline.

**Table 1.** Geometric characteristics of seismic lines.

| Lines | Number of geophones | Geophone spacing (m) | Number of shootings | Total length (m) |
|-------|---------------------|----------------------|---------------------|------------------|
| P0    | 216                 | 3.5                  | 72                  | 756              |
| P1    | 36                  | 3.5                  | 13                  | 126              |
| P2    | 36                  | 3.5                  | 13                  | 126              |
| P3    | 36                  | 3.5                  | 14                  | 126              |

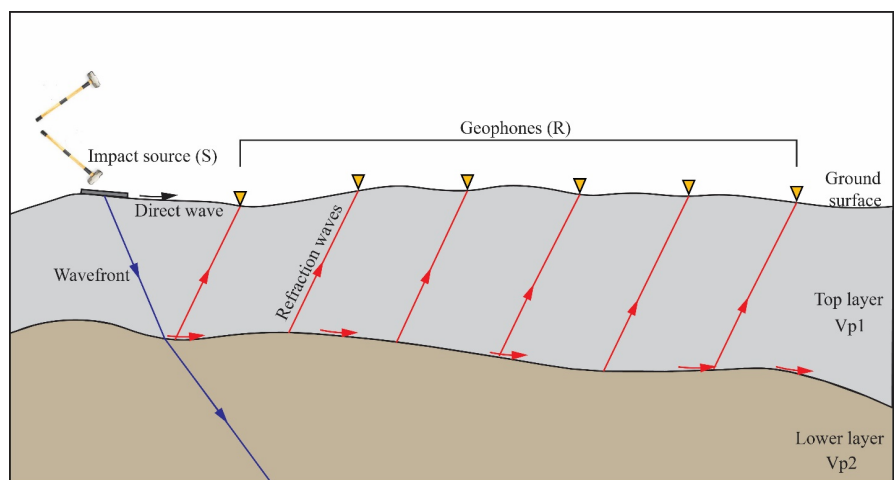


**Figure 3.** Principle of refracted waves propagation.

## 4. Results and Discussion

The results of this study are 2D inverted velocities, representing the distribution of compressional wave velocity  $V_p$ , defining layer thicknesses and the degree of material

rippability as a function of Vp velocities. The spatial distribution of Vp velocities reveals four (04) different geoseismic units. These units range from the lowest densities at the surface to the highest densities at depth. High Vp values are associated with high-density materials, thus quantifying the hardness of the medium and consequently giving an estimate of its degree of rippability. The results obtained show that the formations explored are characterized by velocities ranging from 300 to 5000 m/s. What is more, over the entire study area, all 2D profiles show an increase in Vp velocity with depth, reflecting the existence of increasingly compact formations.

In fact, correlation of 2D isovelocity profiles, *i.e.* the spatial distribution of Vp velocities, with the results of core drilling, shows that surface formations characterized by low Vp values correspond to loose units (topsoil, clay and clayey sands), while sound formations (bedrock) have high Vp values. However, between these two main entities, there are zones of medium velocity corresponding to the altered and/or fractured part of the sound rocks. Classically, loose rock is more rippable than sound rock. These results show that velocity variations in the study area are a clear consequence of variations in lithology and degree of alteration, and hence rippability.

As mentioned above with the existence of four (04) geological units, the combination of the analysis of 2D Vp velocity profiles, the Caterpillar rippability performance chart [17] and especially previous works [18], allowed us to highlight the nature of the different formations according to a color-coded calibration scale based on the Vp velocity distribution (Figure 4).

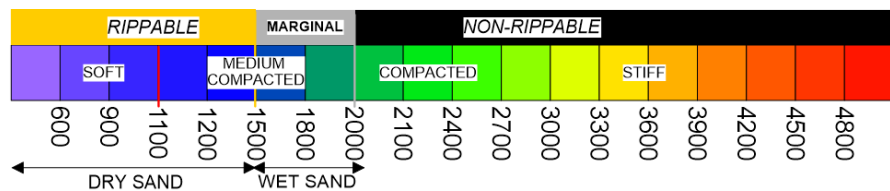


**Figure 4.** Color-coded calibration scale based on Vp velocity distribution.

According to this scale, the first layer of topsoil has a seismic velocity varying between 300 - 900 m/s. This low-velocity zone is rippable and can be found on all three seismic profiles (Figure 5). Other authors such as [19] and [20] have found similar results. Indeed, during work carried out in Malaysia and Senegal respectively, the latter found Vp velocities of between 200 - 800 m/s and 290 - 800 m/s corresponding to overburden. In the case of our study, the slight increase in the Vp velocity of the overburden could be explained by the presence of a lateritic layer in the area. The second unit, made up of weathering products, has a seismic velocity fluctuating between 900 and 2000 m/s. The upper part of this unit is made up of loosely packed formations. Horizons in this unit with a Vp velocity between 900 and 1500 m/s are rippable, while those with a Vp velocity between 1500 and 2000 m/s are marginal (Figure 5). Finally, with a seismic velocity in excess of 3900 m/s, the last geological feature highlighted is a very hard, non-rippable formation (Figure 5). This rock represents the granitic basement. In addition, a horizon characterized by a seismic velocity Vp ranging from 2000 to 3900 m/s constitutes

the fractured part of this basement. This horizon ranges from compact to hard and is also non-rippable.

These various results show that the velocity distribution on 2D seismic profiles is sensitive to lithological variations, the level of compaction and consequently the degree of rippability.

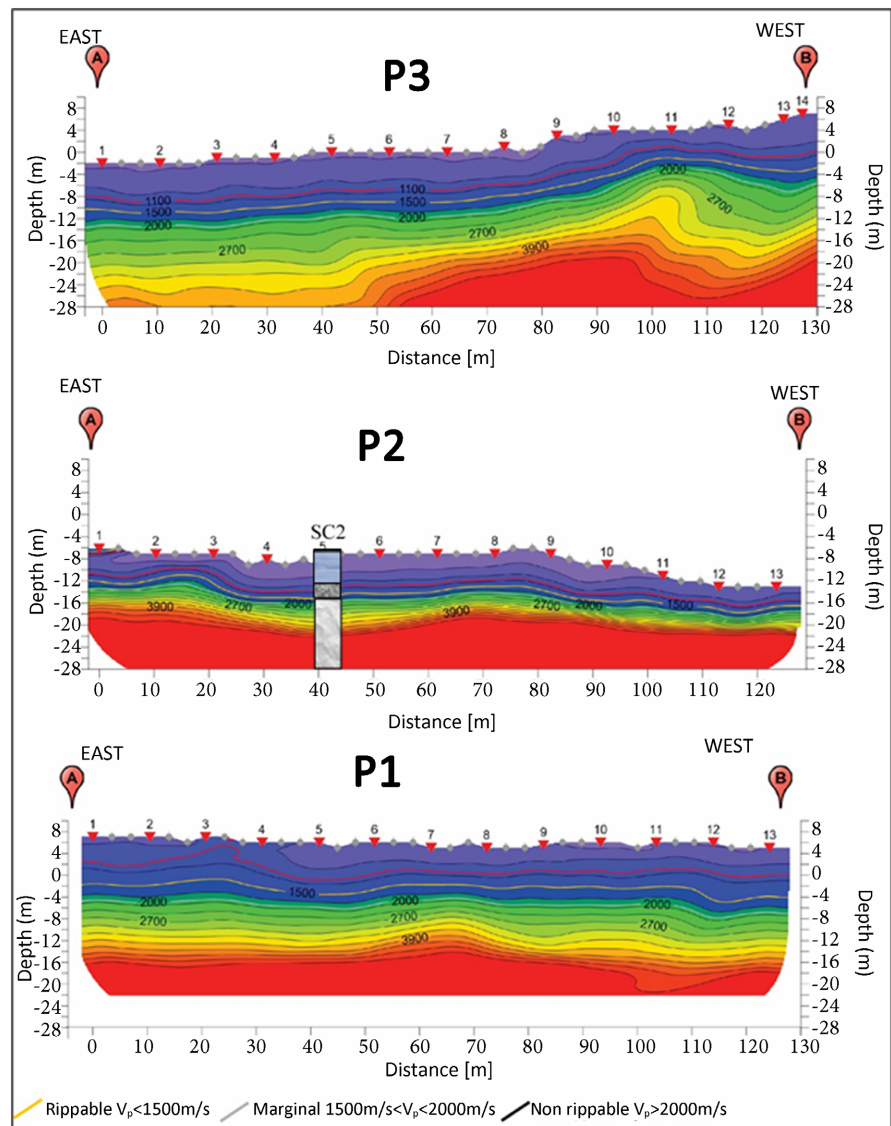


**Figure 5.** 2D inverted seismic refraction geotomographic models.

Indeed, while conducting research in several areas in the Ivorian basement environment, [21] showed that in crystalline basement domains, an alteration lithological series is composed of lateritic cuirass, sandy-clay alterites and fractured basement fringe. These lithological variations were clearly highlighted by the results of the 2D seismic refraction survey, confirmed by the core holes (SC2, SC3 and SC4) (Figure 6) located close to the seismic profiles (P2 and P3).

Based on the synthesis of  $V_p$  seismic velocity data and the SC3 and SC4

geotechnical boreholes, the subsoil in the study area is categorized into rippable (Topsoil, Colorful compact clay marginal) and non-rippable horizons with varying thicknesses. The rippable zone has an average thickness of 6.9 m and appears thicker on profile P1 (Table 2). On this profile, this layer is more or less uniform from east to west over the entire study area (Figure 4). The sediments that predominantly make up this horizon, sands and clays (Figure 6), have a velocity range of between 900 and 1500 m/s. As for the marginal unit, its average thickness is 2.1 m, with a maximum thickness at profile P3 (Table 2). This unit is also dominated by sandy and clayey formations (Figure 6) with a  $V_p$  velocity varying between 1500 and 1800 m/s. This variation in velocity may correspond to the degree of compaction, which generally increases with depth [22].

**Table 2.** Thickness and  $V_p$  velocity of highlighted horizons.

| Velocity $V_p$ (m/s) | Level of rippability | Thickness (m) |     |    |
|----------------------|----------------------|---------------|-----|----|
|                      |                      | P1            | P2  | P3 |
| 300 - 1500           | Rippable             | 9             | 3.7 | 8  |
| 1500 - 2000          | Marginal             | 2             | 1.3 | 3  |
| >2000                | Non-rippable         | -             | -   | -  |

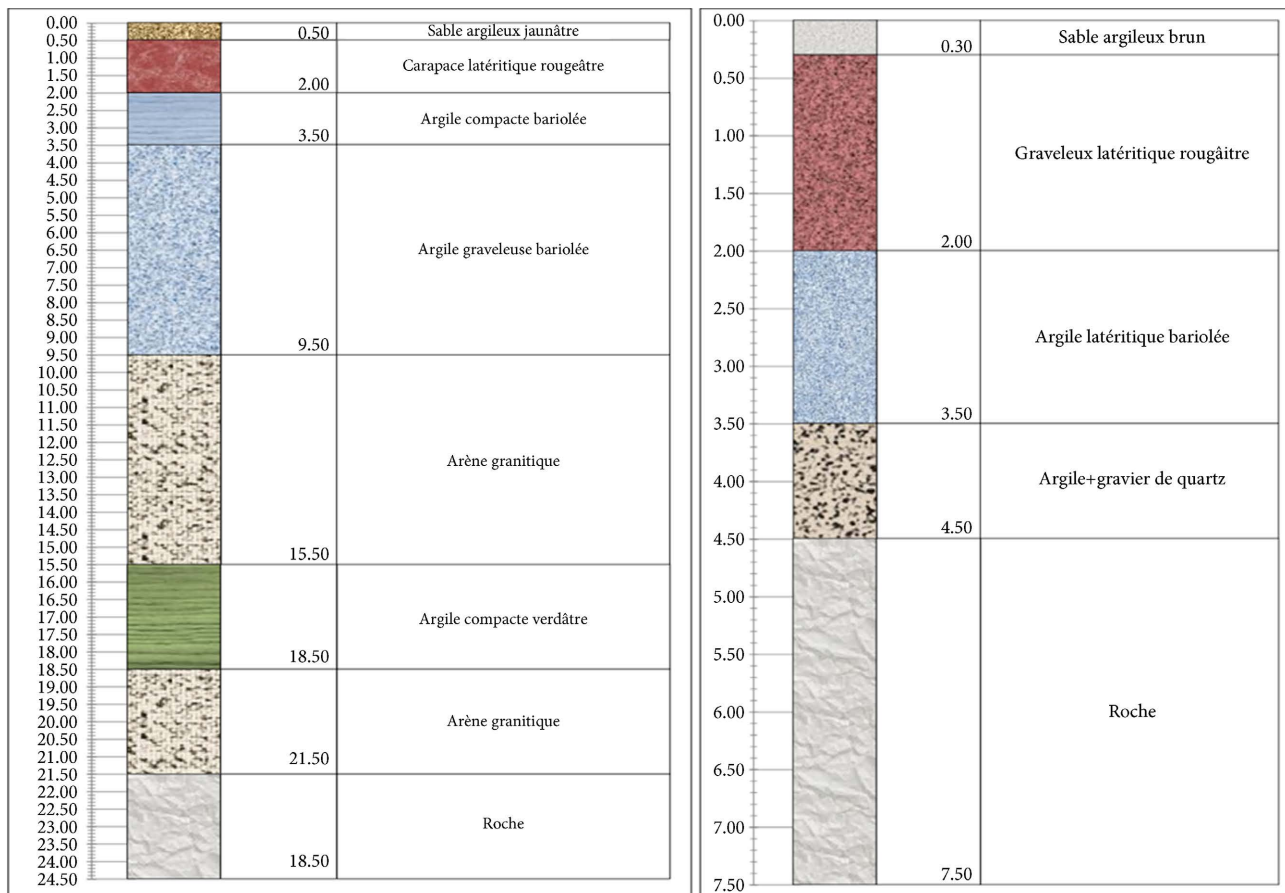


**Figure 6.** Lithological description of core drilling (SC): A (SC2) and B (SC3).

Thus, this variation in velocity and degree of rippability is due to the petrophysical and geotechnical properties of the subsoil formations, mainly the degree of compaction and hardness [19] [23].

Referring to the Caterpillar rippability performance chart [17], the water reservoir should be located in the non-rippable layers, which are between 5 and 11 m deep, according to the geoseismic profiles and core drilling SC2.

## 5. Conclusions

The study of rippable zones in the basement domain in the Kong locality was carried out by analyzing the distribution of compressional wave velocity  $V_p$  calibrated with some nearby core holes. Interpretation of the 2D seismic profiles and core holes revealed four (04) geoseismic units corresponding successively to a low-velocity surface cover, then to weathering products of varying thickness and velocity, and finally to a very dense heterogeneous basement preceded by a zone of fractures and/or fissures. Subsequently, these different geoseismic entities have been categorized into rippable (300 - 1500 m/s), marginal (1500 - 2000 m/s) and non-rippable (>2000 m/s) layers. The rippable horizon lies between 5 and 9 m depth, while the non-rippable fringe lies between 5 and 11 m depth, depending on the profile. Between these two main horizons lie marginal zones with varying degrees of compaction.

Thus, the geological context of the study area presents, at the above-mentioned depths, characteristics conducive to the implementation of a water retention system.

## Conflicts of Interest

The authors declare no conflicts of interest regarding the publication of this paper.

## References

- [1] Bilgili, M., Birirgen, H., Ozbek, A., Ekinici, F. and Demirdelen, T. (2018) The Role of Hydropower Installations for Sustainable Energy Development in Turkey and the World. *Renewable Energy*, **126**, 755-764. <https://doi.org/10.1016/j.renene.2018.03.089>
- [2] Bogaart, P. (2023) The Potential for Sustainable Hydropower. *Nature Water*, **1**, 22-23. <https://doi.org/10.1038/s44221-022-00018-9>
- [3] Castro-Diaz, L., García, M.A., Villamayor-Tomas, S. and Lopez, M.C. (2023) Impacts of Hydropower Development on Locals' Livelihoods in the Global South. *World Development*, **169**, Article 106285. <https://doi.org/10.1016/j.worlddev.2023.106285>
- [4] Meng, Y., Liu, J., Leduc, S., Mesfun, S., Kraxner, F., Mao, G., *et al.* (2020) Hydropower Production Benefits More from 1.5°C than 2°C Climate Scenario. *Water Resources Research*, **56**, e2019wr025519. <https://doi.org/10.1029/2019wr025519>
- [5] Skinner, J., Naisse, M. and Haas, L. (2009) Partage Des Bénéfices Issus Des Grands Barrages En Afrique de l'Ouest. <https://portals.iucn.org/library/node/28678>
- [6] UNIDO (2019) Annual Report 2019. <https://www.unido.org/annualreport2019>
- [7] Lin, P., Huang, B., Li, Q. and Wang, R. (2015) Hazard and Seismic Reinforcement

- Analysis for Typical Large Dams Following the Wenchuan Earthquake. *Engineering Geology*, **194**, 86-97. <https://doi.org/10.1016/j.enggeo.2014.05.011>
- [8] Sigtryggsdóttir, F.G. and Snæbjörnsson, J.T. (2019) Geological Challenges and Geohazard Monitoring of a Mega Engineering Hydropower Project in Iceland. *Engineering Geology*, **259**, Article 105152. <https://doi.org/10.1016/j.enggeo.2019.105152>
- [9] Adamo, N., Al-Ansari, N., Sissakian, V., Laue, J. and Knutsson, S. (2020) Dam Safety: Hazards Created by Human Failings and Actions. *Journal of Earth Sciences and Geotechnical Engineering*, **11**, 65-107. <https://doi.org/10.47260/jesge/1113>
- [10] Inhaber, H. (1980) Risks and Consequences in Energy Production. *Interdisciplinary Science Reviews*, **5**, 304-311. <https://doi.org/10.1179/isr.1980.5.4.304>
- [11] Kostecki, S. and Banasiak, R. (2021) The Catastrophe of the Niedów Dam—The Causes of the Dam's Breach, Its Development, and Consequences. *Water*, **13**, Article 3254. <https://doi.org/10.3390/w13223254>
- [12] Leffer, L. (2023) Dams Worldwide Are at Risk of Catastrophic Failure. Scientific American. <https://www.scientificamerican.com/article/dams-worldwide-are-at-risk-of-catastrophic-failure/>
- [13] Sivapriya, S.V. and Anne Sherin, A. (2021) Causes and Consequences of Dam Failures—Case Study. In: *Lecture Notes in Civil Engineering*, Springer, 155-159. [https://doi.org/10.1007/978-981-16-5041-3\\_11](https://doi.org/10.1007/978-981-16-5041-3_11)
- [14] Sovacool, B.K., Kryman, M. and Laine, E. (2015) Profiling Technological Failure and Disaster in the Energy Sector: A Comparative Analysis of Historical Energy Accidents. *Energy*, **90**, 2016-2027. <https://doi.org/10.1016/j.energy.2015.07.043>
- [15] Soro, Y.G.P., Toure, M. and Aka, A.F. (2022) L'impact du barrage hydroélectrique de Soubré dans le sud-ouest de la Côte d'Ivoire. Regardsuds, EDUCI. <https://regardsuds.org/limpact-du-barrage-hydroelectrique-de-soubre-dans-le-sud-ouest-de-la-cote-divoire/>
- [16] Bernus, E. (1960) Kong et Sa Région. <https://www.semanticscholar.org/paper/Kong-et-sa-r%C3%A9gion-Bernus/335f34324180751ad97ab00fe3d66482d78c1b45>
- [17] Caterpillar (2019) Caterpillar Performance Handbook. <https://www.macallister.com/Parts-service/Caterpillar-performance-handbook/>
- [18] Mavko, G., Mukerji, T. and Dvorkin, J. (2009) The Rock Physics Handbook. 2nd Edition, Cambridge University Press. <https://doi.org/10.1017/cbo9780511626753>
- [19] Akingboye, A.S. and Bery, A.A. (2022) Characteristics and Rippability Conditions of Near-Surface Lithologic Units (Penang Island, Malaysia) Derived from Multimethod Geotomographic Models and Geostatistics. *Journal of Applied Geophysics*, **204**, Article 104723. <https://doi.org/10.1016/j.jappgeo.2022.104723>
- [20] Ndiaye, M., Sall, O.A., Thiam, A., Sarr, D., Badji, M. and Ndoye, I. (2020) Investigating the Depth and the Geometry of the Quarzitic Panafrican Basement Using Near-Surface 3D Seismic Refraction Tomography: Case Study of the Locality of Bakel (Senegal). *International Journal of Geosciences*, **11**, 345-359. <https://doi.org/10.4236/ijg.2020.116018>
- [21] Sombo, A.P., Kouakou, K.E.G., Kouassi, F.W., Koudou, A. and Bie, G.R. (2017) Profil d'altération et Potentiel Aquifère En Zone de Socle Cristallin Au Sud de La Côte d'Ivoire. *International Journal of Innovation and Applied Studies*, **19**, 919-928. <https://issr-journals.org/xplore/ijias/0019/004/IJIAS-16-227-13.pdf>
- [22] Uyanik, O. and Ulugergerli, E.U. (2007) Quality Control of Compacted Grounds

Using Seismic Velocities. *Near Surface Geophysics*, **6**, 299-306.

<https://doi.org/10.3997/1873-0604.2008004>

- [23] Jug, J., Stanko, D., Grabar, K. and Hrženjak, P. (2020) New Approach in the Application of Seismic Methods for Assessing Surface Excavatability of Sedimentary Rocks. *Bulletin of Engineering Geology and the Environment*, **79**, 3797-3813.

<https://doi.org/10.1007/s10064-020-01802-1>